Density Functional Study on the Effect of the trans Axial Ligand of B_{12} Cofactors on the Heterolytic Cleavage of the Co−C Bond

Nicole Dölker, Feliu Maseras,* and Agustí Lledós

Unitat de Química Física, Edifici C.n, Universitat Autònoma de Barcelona, 08193 Bellaterra, Catalonia, Spain

Received: June 4, 2002; In Final Form: September 13, 2002

Density functional theory (DFT) Becke3LYP calculations including full and restricted geometry optimizations are carried out on the complex $[Co(Cor)(Benz)(CH_3)]^+$ (Cor = corrin, Benz = benzimidazole), which is a model of B_{12} cofactors, and on the products of the two possible heterolytic cleavages of the Co−C bond, $[Co(Cor)(Benz)(CH_3)]$, CH_3^+, $[Co(Cor)(Benz)(CH_3)]^{2+}$, and CH_3^-. The thermodynamics of the heterolytic processes are found to depend very significantly on the distance of the axial ligand from the cobalt. The results are explained through simple molecular orbital reasonings, and their possible implications for the biological reactivity of adenosylcobalamin and methylcobalamin are discussed.

1. Introduction

Cobalt(III) corrins are the main structural motif of B_{12} cofactors,[1,2] which are central to the enzymatic catalysis of two different biologically relevant reactions: isomerization through radical intermediates and methyl transfer. Enzymes catalyzing rearrangements,[3] such as methylmalonyl-CoA mutase,[4] use adenosylcobalamin (Figure 1) as a cofactor, and its main mechanistic feature appears to be the homolytic cleavage of the Co−C bond, which gives rise to a Co(II) complex and an adenosyl radical. Methyltransferases[5] such as methionine synthase[6] use methylcobalamin (Figure 1) as a cofactor and present as a characteristic reaction step the heterolytic cleavage of the Co−C bond to produce Co(I) and a formal CH_3^+ group, which is immediately bound elsewhere.

The detailed mechanism of either of the two reactions is still not completely understood; therefore, they are subject to active experimental work. Intense research activity is taking place in a number of directions, such as the behavior of the enzymes themselves,[7,8] that of isolated cobalamins,[9] and that of related models such as other cobamides,[10] cobaloximes,[11] and related systems.[12−14] Experiments on B_{12} cofactors have traditionally been on the leading edge of the application of novel experimental techniques[15] and continue to be so in fields such as photoacoustic calorimetry,[16] cryogenic resonance Raman,[17] EXAFS,[18] EPR,[19] and time-resolved photolysis.[20] In fact, the interpretation of a number of experimental measurements is still subject to discussion.[18,19,21−23]

The main problems in the experimental study of these systems are the complexity and variety of factors involved and the difficulties inherent in their accurate evaluation. Because of this, theoretical calculations can provide a complementary and helpful tool. Computational approaches start necessarily with a simplification of the system; therefore, they can target the role of one particular property of the system in the reaction mechanism. Of course, the risk can be oversimplification, and theoretical conclusions must be critically evaluated in conjunction with experimental data.

Computational studies with a variety of methods have been carried out on B_{12} cofactors. Molecular mechanics have been applied by several authors.[24−29] This method is appropriate for discussing the steric effects of distortions in the corrin ring and its interaction with axial ligands but struggles with the introduction of electronic effects, requiring a very precise tuning of the force field, which is not always possible. Methods based on quantum chemistry can certainly introduce electronic effects more accurately in biochemistry,[30] but their application has been difficult until very recently because of the large size of the system and its intrinsic complexity. Because of this, early studies could obtain only qualitative conclusions.[31−34] Applications based on density functional theory (DFT) have recently allowed for the drawing of quantitative conclusions on B_{12} cofactors and their reactivity. ^{14}N superhyperfine and nuclear quadrupole coupling constants have been estimated,[35,36] and the substrate radical-to-product radical rearrangement reactions in adenosylcobalamin-dependent enzymes have been analyzed.[37−40] Accurate DFT studies have also examined the stereoelectronic properties of cobalamin derivatives.[41−45]

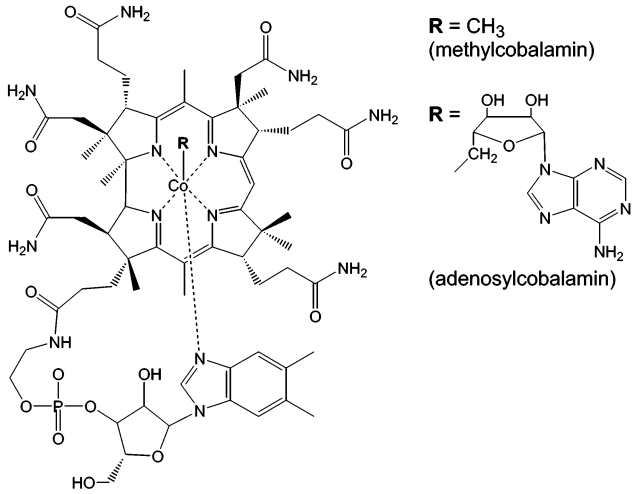

Figure 1. Structure of the cobalamin cofactors.

These DFT studies on B_{12} cofactors and related species were focused on structural aspects and on their relationship to the homolytic Co−C bond dissociation process characteristic of the B_{12} coenzyme. In particular, we analyzed the effect of the distance between cobalt and the axial ligand trans to the Co−C

* Corresponding author. E-mail: feliu@klingon.uab.es.

10.1021/jp026233p CCC: $25.00
Published on Web 12/10/2002

bond (Figure 1) on this homolytic cleavage.[45] The eventual role of this ligand is one of the most studied and uncertain mechanistic aspects of the enzymatic process.[15] The reaction that was studied was[45]

$$[Co(Cor)(Benz)(CH_3)]^+ \rightarrow [Co(Cor)(Benz)]^+ + CH_3$$

The conclusion was that the distance of the trans axial ligand from the Co has very little effect on the thermodynamics or kinetics of the homolytic cleavage, a result that seems to be in agreement with recent experimental observations.[19,46] Other studies in which the character of the axial ligand rather than the $Co-N_{axial}$ distance is varied show an inverse trans effect.[41,42] This effect is nevertheless quite small, and, in any case, recent experimental results indicate that such an inverse trans influence is not a general feature of cobalamins.[47] A different role of the axial ligand—preventing heterolysis—in enzymes carrying out homolysis has been proposed.[12,32] This aspect could not be analyzed with the study of the homolysis alone but requires the study of the heterolysis reaction.

In the present article, we intend to analyze with the same DFT method the role of the distance of the axial base from the cobalt in heterolytic cleavage. This reaction is catalyzed by methyltransferases,[5] where the cofactor is methylcobalamin (Figure 1). To our knowledge, this process has not been studied previously with high-level quantum chemistry methods. Apart from the comparison with homolysis mentioned above, the study of heterolysis is interesting in itself. In fact, experimental data suggest a more likely involvement of the axial ligand in heterolysis than in homolysis. Whereas the original dimethylbenzimidazole group of cobalamin remains attached to the cobalt in a number of enzymes performing homolysis[36,48−50] (though not in all of them[4,51]), this is never the case for the characterized enzymes carrying out heterolysis.[6,52−54] In most of these cases, the dimethylbenzimidazole axial ligand is replaced by a histidine from the protein chain. This enhances the potential role of the protein in the modulation of the cleavage reaction by introducing changes in the position of the axial base.[54] However, the direct correlation between the distance of the axial ligand from the Co and the ease of heterolytic cleavage has not been proved yet.

We are going to consider the two possible heterolytic scissions of the Co−C bond in $[Co(Cor)(Benz)(CH_3)]^+$ (Cor = corrin, Benz = benzimidazole), which will be labeled arbitrarily as A and B:

$$[Co(Cor)(Benz)(CH_3)]^+ \rightarrow [Co(Cor)(Benz)] + CH_3^+ \quad (A)$$

$$[Co(Cor)(Benz)(CH_3)]^+ \rightarrow [Co(Cor)(Benz)]^{2+} + CH_3^- \quad (B)$$

Reaction A corresponds to the heterolytic cleavage observed in biological environments, in which Co(III) goes to Co(I). The CH_3^+ leaving group does not stay as such but is immediately transferred to another group, homocysteine to produce methionine in the case of methionine synthase. Reaction B corresponds to a somehow more intuitive heterolytic cleavage of the bond, with both electrons going to the more electronegative atom, carbon. In reaction B, there is no change in the oxidation state—the cobalt remains Co(III)—and there is a departure of CH_3^-. In biological environments, however, reaction B takes place only as a side reaction that leads to the degradation of the cofactor.[12,16,23,55]

Therefore, the present study on the effect of the axial base on Co−C bond heterolysis has a dual goal affecting both types of B_{12} cofactors. In the case of enzymes carrying out rearrangements, we hope that the current study will clarify the eventual role of the axial ligand in preventing heterolytic cleavage. For the case of methyltransferases, we intend to analyze to what extent displacements of the axial base can modulate the reactivity of the cofactor.

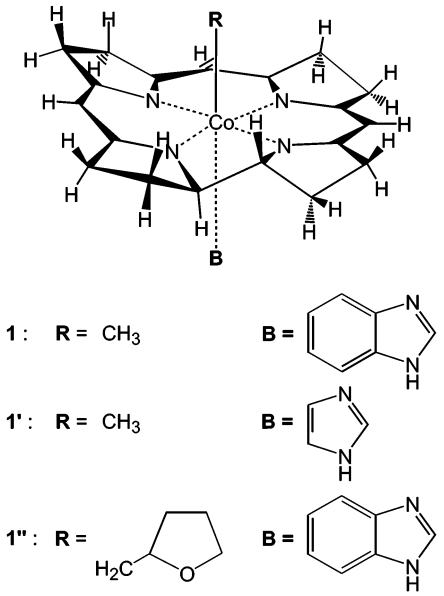

Figure 2. Models for methylcobalamin with benzimidazole as an axial ligand, $[Co(Cor)(Benz)(CH_3)]$ (**1**), methylcobalamin with histidine as an axial ligand, $[Co(Cor)(Im)(CH_3)]$ (**1′**), and adenosylcobalamin, $[Co(Cor)(Benz)(CH_2R)]$ (R = tetrahydrofuran) (**1″**), used in this work.

2. Computational Details

All calculations have been carried out using the Becke3LYP method.[56−59] Two different basis sets have been used. Most calculations have been carried out with basis set I. In basis set I, the 10 innermost electrons of Co have been replaced by a quasi-relativistic effective core potential, and the valence electrons have been described by the corresponding LANL2DZ basis set.[60] For the atoms bonded directly to the metal center, the 6-31G* basis[61,62] has been used, whereas all other atoms have been described by the STO-3G basis.[63] Some additional single-point calculations have been carried out with basis set II by using a LANL2DZ basis plus polarization[64] for Co and a 6-31G* basis for all other atoms. All calculations have been performed with the Gaussian 98 program package.[65]

Figure 2 shows the models used in the present study. The $[Co(Cor)(Benz)(CH_3)]^+$ (Cor = corrin, Benz = benzimidazole) model for methylcobalamin (**1**) includes the unsubstituted corrin ring and a benzimidazole molecule as the axial base. Methylcobalamin with a histidine residue as the axial ligand is modeled by $[Co(Cor)(Im)(CH_3)]^+$ (Im = imidazole) (**1′**). In the $[Co(Cor)(Benz)(CH_2R)]^+$ (R = tetrahydrofuran) model for adenosylcobalamin (**1″**), the adenosyl group has been modeled by a methyl group substituted with a tetrahydrofuran ring.

3. Results

3.1. Geometry Optimizations. Full geometry optimizations at the Becke3LYP level of theory have been performed on a number of different compounds: our model for methylcobalamin $[Co(III)(Cor)(Benz)(CH_3)]^+$ (**1**) and the products of Co−C bond homolysis $[Co(II)(Cor)(Benz)]^+$ (**2**) and CH_3 as well as the products of the two possible Co−C bond heterolysis reactions discussed in the Introduction—type A, yielding [Co-

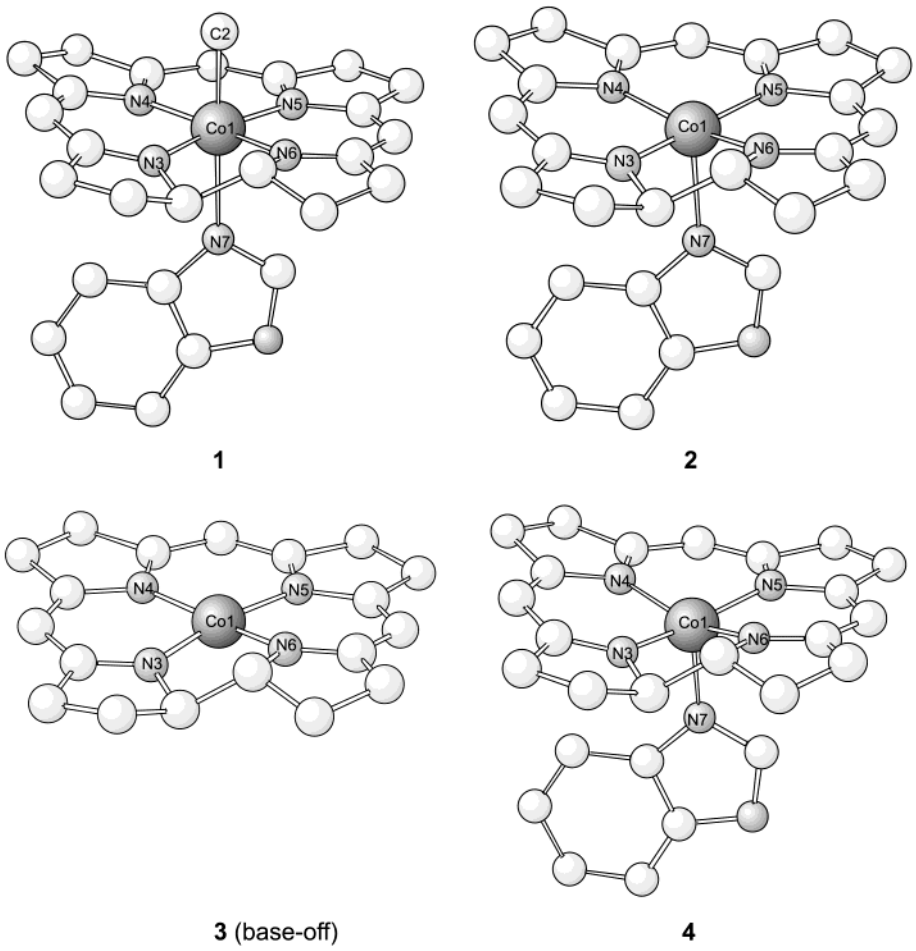

Figure 3. Becke3LYP optimized structures of methylcobalamin (**1**), the product of Co−C bond homolysis (**2**), and the heterolysis products cob(I)alamin **3**(base-off) and cob(III)alamin **4**. Hydrogen atoms have been omitted for simplicity.

TABLE 1: Selected Geometry Parameters for the Four Optimized Structures of Methylcobalamin (1) and the Products of Homolysis (2) and Heterolysis (3, base-off, and 4) (in Å and deg)[a]

compound	**1**	**2**	**3** (base-off)	**4**
d(Co−C2)	1.961 (1.99(2))			
d(Co−N3)	1.908 (1.88(2))	1.909	1.871	1.904
d(Co−N4)	1.948 (1.97(2))	1.958	1.927	1.948
d(Co−N5)	1.951 (1.93(2))	1.953	1.927	1.947
d(Co−N6)	1.905 (1.89(2))	1.914	1.871	1.904
d(Co−N7)	2.288 (2.19(2))	2.296		1.928
∠(N7,Co,C2)	177.57 (171(2))			
∠(N7,Co,N3)	88.44 (93(2))	93.48		96.01
∠(N7,Co,N4)	91.73 (89(2))	97.90		103.33
∠(N7,Co,N5)	87.53 (86(2))	91.34		94.28
∠(N7,Co,N6)	91.28 (95(2))	97.22		99.11
∠(C2,Co,N3)	93.95 (95(2))			
∠(C2,Co,N4)	87.76 (86(2))			
∠(C2,Co,N5)	90.15 (87(2))			
∠(C2,Co,N6)	89.52 (90(2))			

[a] X-ray data for the crystal structure related to **1**[81] are shown in parentheses. Atom labels are shown in Figure 3.

(I)(Cor)(Benz)] (**3**) and CH_3^+ and type B, yielding [Co(III)(Cor)(Benz)]$^{2+}$ (**4**) and CH_3^-. Figure 3 shows the computed equilibrium structures for the corrin systems. Selected geometry parameters of the structures in Figure 3 are listed in Table 1. The geometry parameters of model compound **1** and the product of homolysis **2** have already been discussed in a previous work.[45] **1** shows a nearly octahedral coordination geometry. The cobalt center lies 0.008 Å above the mean square formed by the four equatorial nitrogens. The geometry parameters computed for **1** are in good agreement with the X-ray data for free methylcobalamin. The only discrepancy appears in the Co−N_{ax} distance, where the computed value of 2.29 Å is 0.1 Å longer than the experimental value (2.18 Å). In recent studies on a variety of cobalamin compounds, other authors find the same difference between calculations and experiment for all of the structures taken into account.[41,43] The reason for this discrepancy is probably related to the fact that all of the models studied theoretically lack the linking sidearm that connects the axial ligand to the corrin ring. The overestimation of the Co−N_{ax} bond length in the computed structures, however, is of no importance for the trends discussed in this work.

When comparing the geometries of **1** and **2**, no important changes are found. The bonds between the metal center and the equatorial ligands are lengthened by less than 0.01 Å, and the cobalt moves 0.17 Å out of the mean-square plane formed by the equatorial nitrogens and is slightly displaced toward the axial benzimidazole.

The geometry of the products of both types of heterolysis of the Co−C bond shows more important changes. The product of heterolysis of type A, in which both electrons are left on cobalt to form cob(I)alamin, was found to be unstable in its five-coordinate form [Co(I)(Cor)(Benz)] **3**(base-on). The stable four-coordinate compound [Co(I)(Cor)] **3** (base-off) has C_2 symmetry with the cobalt located in the center of the mean-square plane of the equatorial nitrogens. All cobalt−nitrogen bonds are shortened noticeably with respect to six-coordinate compound **1** (between 0.020 and 0.038 Å).

TABLE 2: Absolute Co−C Bond Dissociation Energies for Homolysis and Both Types of Heterolysis at Fixed Co−N_{ax} Distances (in kcal/mol)

R(Co−N_{ax})	homolysis	heterolysis type A	heterolysis type B
1.80	24.0	221.9	238.8
2.00	23.4	219.9	250.0
2.20	23.0	213.9	259.4
2.29	22.9	211.2	262.9
2.40	23.0	207.8	267.3
2.60	23.4	203.1	
2.80	23.9	199.7	

Heterolysis of type B, in which both electrons are left on the carbon, leads to the formation of the five-coordinate cob(III)-alamin **4** and CH_3^-. In this case, the most remarkable changes in the geometry of the cobalamin are the 0.267-Å displacement of the cobalt out of the mean-square plane of the equatorial nitrogens toward the axial benzimidazole and the shortening of the Co−N_{ax} bond by 0.356 Å (1.928 Å compared to 2.29 Å in **1**). The Co−N_{eq} bonds, on the contrary, are changed by less than 0.005 Å with respect to those of **1**.

3.2. Thermodynamics of the Heterolytic Co−C Bond Cleavage. As mentioned in the Introduction, it has been shown previously that the influence of the distance between the cobalt center and the axial ligand on the thermodynamics and kinetics of the homolytic Co−C bond cleavage is minimal. To study the possible effect of the Co−N_{ax} distance on both types of Co−C bond heterolyses, we have carried out restricted geometry optimizations of reactants and products with frozen Co−N_{ax} distances.

Formation of cob(I)alamin. Enzymes that depend on methylcobalamin as a cofactor catalyze methyl transfer reactions in which the Co−C bond is cleaved heterolytically such that CH_3^+ is formed and both electrons are left on cobalt to give cob(I)-alamin (heterolysis type A). We have calculated the corresponding bond dissociation energy (BDE) as the energy of the reactions of type

$$\mathbf{1}(\text{frozen } R(\text{Co}-\text{N}_{ax}))^+ \rightarrow \mathbf{3}(\text{frozen } R(\text{Co}-\text{N}_{ax})) + \text{CH}_3^+$$

where the frozen Co−N_{ax} distance is the same for **1** and **3**. It has been varied between 1.8 and 2.8 Å in steps of 0.1 Å.

This type of reaction that leads to the formation of isolated CH_3^+ is very endothermic. In particular, the reaction energy when considering the fully optimized forms of all species involved (when the axial ligand is dissociated from cob(I)-alamin) is 194.3 kcal/mol. These large values are nevertheless not chemically relevant because in biological systems the CH_3^+ will not stay as such but will immediately be bound elsewhere. This aspect will be discussed in detail later in this article. In any case, the change in the endothermicity of this reaction as a response to displacements of the trans axial ligand will be significant. Because of this, in the assumptions that follow as well as in the corresponding figures, we will not use the absolute BDE, which can nevertheless be found in Table 2, but a relative BDE that is defined as the difference in the absolute BDE for a particular Co−N_{ax} distance with respect to the value associated with the equilibrium Co−N_{ax} distance for the corresponding six-coordinate compound. In the current case, the equilibrium distance is 2.29 Å, and the associated absolute BDE is 211.2 kcal/mol, which is therefore used as the origin of relative BDEs.

Figure 4 shows the dependence of the reaction energy of the heterolytic Co−C bond cleavage with respect to the Co−N_{ax} distance (circles). It can be seen that the Co−C BDE changes quite dramatically when the distance of the axial ligand from the Co is changed. A shortening of the Co−N_{ax} distance by 0.5 Å with respect to the optimal value in **1** of 2.29 Å leads to an increase in the Co−C BDE of more than 10 kcal/mol. Lengthening of the Co−N_{ax} distance by 0.5 Å, on the contrary, results in a decrease of the dissociation energy of 11 kcal/mol. Because the BDE for Co−C bond homolysis depends very little on the Co−N_{ax} distance,[45] it can be concluded that lengthening of the Co−N_{ax} bond favors type A heterolysis over homolysis. At short Co−N_{ax} distances, however, type A heterolysis is less feasible.

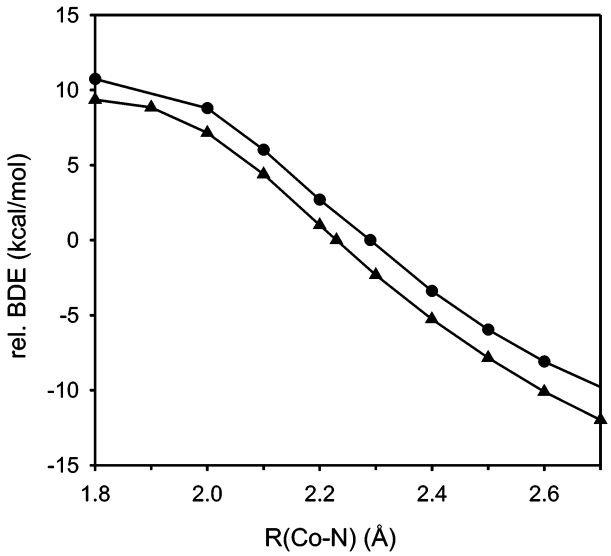

Figure 4. Relative Co−C bond dissociation energy (in kcal/mol) for the formation of cob(I)alamin. Two curves are shown, corresponding to benzimidazole (●) and histidine (▲) as axial ligands. The bond dissociation energies at the optimal Co−N_{ax} distance in **1** (2.29 Å) and **1′** (2.23 Å) have been chosen as zero. The absolute BDE in the gas phase at the optimal Co−N_{ax} distance is 211.2 kcal/mol for **1** and 214.4 for **1′**.

These results can be better understood if the BDE is decomposed into the components associated with the reactant and the product. In Figure 5, the relative energies of **1** (solid line) and **3** + CH_3^+ (dashed line) are plotted as a function of the Co−N_{ax} distance. Again, for the sake of readability, relative energies in kcal/mol are presented relative to the value at a Co−N_{ax} distance of 2.29 Å (−1507.6403 hartrees for **1** and −1507.3038 hartrees for **3** + CH_3^+), which has been chosen as zero for each curve to make the dependence of the energy on the Co−N_{ax} distance more easily comparable. It can be seen that the energy of six-coordinate compound **1** is not affected very much by a lengthening of the Co−N_{ax} distance. Also, a shortening by up to 0.3 Å leads only to a relatively small increase in energy (3.8 kcal/mol). Only when the Co−N_{ax} distance is shortened by more than 0.3 Å does the energy of **1** increases significantly. The energy of cob(I)alamin **3**, however, is very sensitive to the Co−N_{ax} distance. In the gas phase, **3** is not stable but dissociates spontaneously to four-coordinate compound **3**(base-off) and free benzimidazole. Therefore, its energy decreases dramatically when the Co−N_{ax} distance is lengthened and increases much faster than that of **1** when the Co−N_{ax} distance is shortened. The energy of **3** changes by as much as 37 kcal/mol when the Co−N_{ax} distance changes from 1.8 to 2.8 Å. It can be summarized that upon a lengthening of the Co−N_{ax} distance the energy of the reactant (**1**) is not affected very much whereas the product (**3**) is stabilized, which leads to a decrease in the reaction energy. Shortening of the Co−N_{ax} bond destabilizes both the reactant and the product. The product, however, is much more affected, so the reaction energy increases.

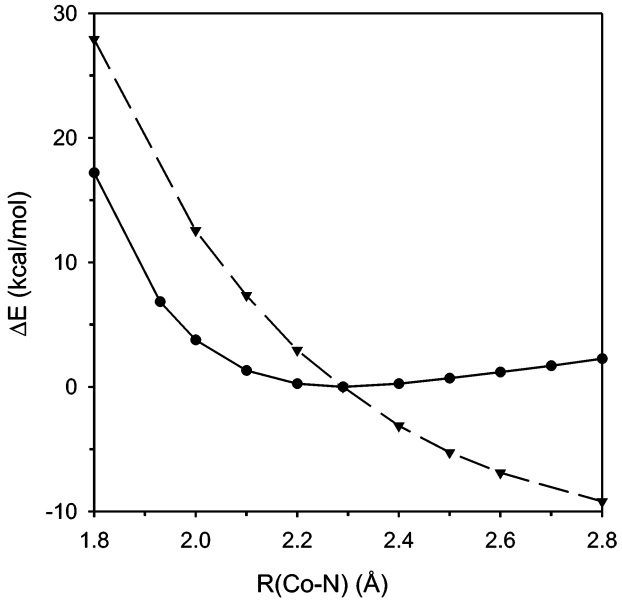

Figure 5. Relative energy (in kcal/mol) of **1** (—) and **3** + CH_3^+ (– –) as a function of the Co−N_{ax} distance (in Å). The energies at the optimal Co−N_{ax} distance in **1** (2.3 Å) have been chosen as zero for both curves. The absolute energies at this point are −1507.6403 hartrees for the reactant and −1507.3038 hartrees for the product.

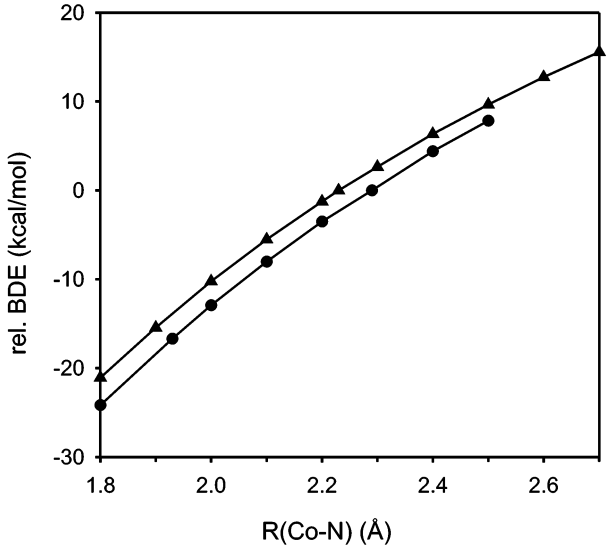

Figure 6. Relative Co−C bond dissociation energy (in kcal/mol) for the formation of cob(III)alamin. Two curves are shown, corresponding to benzimidazole (●) and histidine (▲) as axial ligands. The bond dissociation energies at the optimal Co−N_{ax} distance in **1** (2.29 Å) and **1′** (2.23 Å) have been chosen as zero. The absolute BDE in the gas phase at the optimal Co−N_{ax} distance is 262.9 kcal/mol for **1** and 263.1 for **1′**.

The dependence of the reaction energy of the heterolytic cleavage of the Co−C bond, which leads to the formation of cob(I)alamin, on the distance between the cobalt center and the axial benzimidazole ligand is therefore due to a stabilization of the product at long distances and its destabilization at short Co−N_{ax} distances.

Formation of cob(III)alamin. A second mode of heterolytic Co−C bond cleavage has been observed as a side reaction in the thermolysis and photodissociation of free adenosylcobalamin. In this case, both electrons are left on the alkyl group, and cob(III)alamin and products derived from adenosyl are formed.[12,16,23,66]

To study the influence of the axial ligand on this type of Co−C bond heterolysis (type B), we have considered reactions of the type

$$\mathbf{1}(\text{frozen } R(\text{Co}-\text{N}_{ax}))^{+} \rightarrow \mathbf{4}(\text{frozen } R(\text{Co}-\text{N}_{ax}))^{2+} + \text{CH}_3^{-}$$

The frozen value is always the same for **1** and **4** and has been varied in steps of 0.1 Å between 1.8 and 2.5 Å.

Figure 6 shows the dependence of the reaction energy on the Co−N_{ax} bond length (circles). The absolute bond dissociation energies are shown in Table 2. It can be seen that, contrary to what was found for the formation of cob(I)alamin, the formation of five-coordinate cob(III)alamin is strongly favored by a short Co−N_{ax} distance. If the Co−N_{ax} bond is shortened by 0.5 Å, then the BDE is lowered by 24 kcal/mol. A lengthening of the Co−N_{ax} bond by 0.2 Å, however, leads to an increase of 7.8 kcal/mol in the dissociation energy for the Co−C bond. Decomposition of the dissociation energy in the energies corresponding to the reactant and the products (Figure 7) shows that the increase in the BDE upon shortening of the Co−N_{ax} bond is due to the fact that the five-coordinate cob(III)alamin has an energy minimum at the short Co−N_{ax} distance of 1.93 Å and is strongly destabilized when the Co−N_{ax} bond is lengthened. If the Co−N_{ax} bond becomes shorter than 1.93 Å, then the energy of **4** increases. The energy of six-coordinate compound **1**, however, is even more strongly affected by a

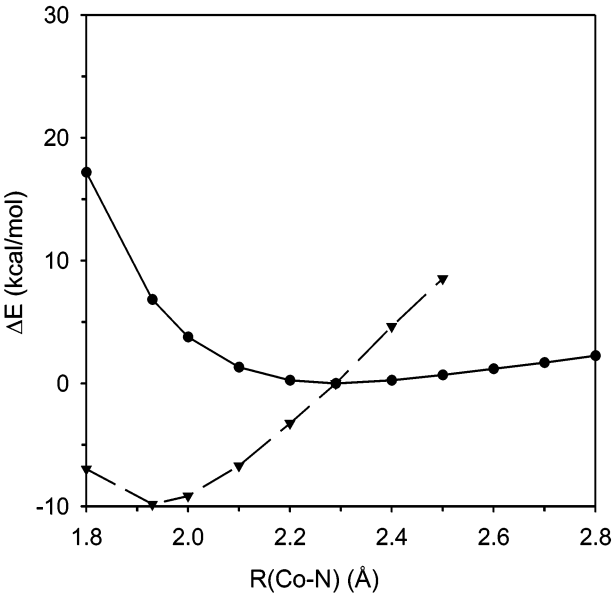

Figure 7. Relative energy (in kcal/mol) of **1** (—) and **4** + CH_3^- (– –) as a function of the Co−N_{ax} distance (in Å). The energies at the optimal Co−N_{ax} distance in **1** (2.29 Å) have been chosen as zero for both curves. The absolute energies at this point are −1507.6403 hartrees for the reactant and −1507.2213 hartrees for the product.

shortening of the Co−N_{ax} distance so that at a Co−N_{ax} distance of 1.8 Å the formation of **4** takes place more easily than at a distance of 2.29 Å, which is optimal for **1**. At short Co−N_{ax} distances, type B heterolysis would therefore be favored over homolysis of the Co−C bond. The idea of the role of the trans ligand in preventing the coenzyme from undesired side reactions[66−68] has recently gained support from the observation that substitution of the axial benzimidazole by a cyanide ligand leads to type B heterolysis of the Co−C bond.[69,70] Cyanide is a very strong σ-electron donor. Therefore, the exchange of benzimidazole for cyanide has the same effect as a shortening of the Co−N_{axial} bond: the electron density on cobalt is increased.

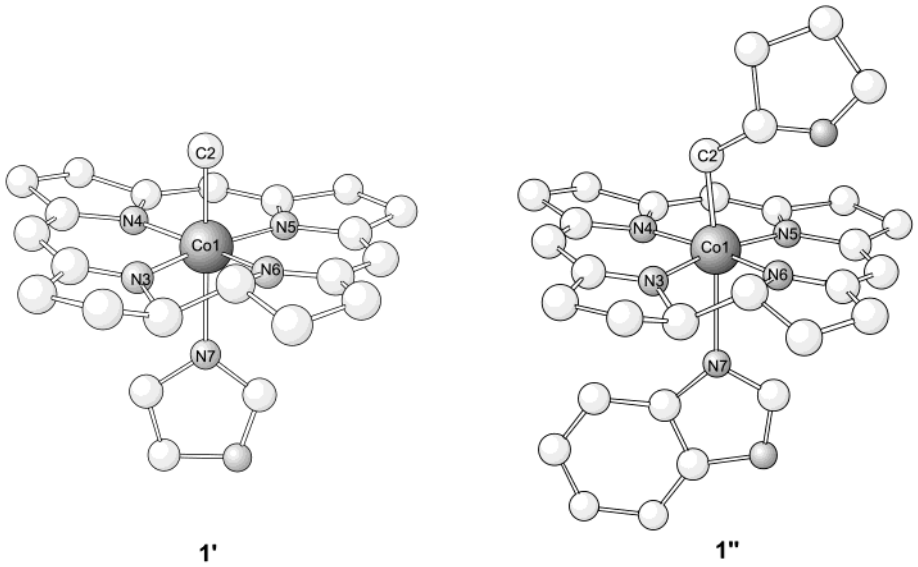

Figure 8. Becke3LYP optimized structures of our model for methylcobalamin with histidine as an axial ligand (**1′**) and adenosylcobalamin (**1″**).

3.3. Histidine as the Axial Ligand. In the enzymatic environment, in some cases, the axial dimethylbenzimidazole ligand is replaced by a histidine from a protein side chain.[36,48−50] To study the possible influence of this ligand change on the thermodynamics and kinetics of the enzymatic catalysis, the heterolytic Co−C bond cleavage has also been studied for a model system in which the benzimidazole has been replaced by unsubstituted imidazole, which should be a valid model for histidine. The model system $[Co(Cor)(Im)(CH_3)]^+$ (**1′**) has been fully optimized in the singlet state at the Becke3LYP level of theory. The optimized structure is shown in Figure 8. The geometric parameters of **1′** have been discussed previously.[45] The structure of **1′** closely resembles that of **1**, the only noticeable difference being the Co−N_{ax} distance, which is 0.057 Å shorter in **1′** than in **1** (2.230 Å instead of 2.29 Å). The Co−C bond distance, however, is not affected by the ligand change, and the dissociation energy for a homolytic cleavage changes by less than 1 kcal/mol (23.7 kcal/mol in **1′** instead of 22.9 kcal/mol in **1**).

The reaction energy for both heterolytic Co−C bond cleavage processes in **1′** has been calculated as the energy of the reactions

$$\mathbf{1'}(\text{frozen } R(\text{Co}-\text{N}_{ax}))^+ \rightarrow \mathbf{3'}(\text{frozen } R(\text{Co}-\text{N}_{ax})) + \text{CH}_3^+$$

and

$$\mathbf{1'}(\text{frozen } R(\text{Co}-\text{N}_{ax}))^+ \rightarrow \mathbf{4'}(\text{frozen } R(\text{Co}-\text{N}_{ax}))^{2+} + \text{CH}_3^-$$

as has been described previously for **1**. **3′** and **4′** are the heterolysis products in which the axial coordination site is occupied by imidazole. The formation of **3′** has been studied for Co−N_{ax} bond lengths in the range between 1.8 and 2.7 Å, and the formation of **4′**, between 1.8 and 2.5 Å. In both cases, the Co−N_{ax} bond length has been varied in steps of 0.1 Å.

Formation of cob(I)alamin. Figure 4 shows the relative reaction energies for type A heterolysis, the operation mode of methylcobalamin in biological systems. The dependence of the bond dissociation energy of **1′** on the Co−N_{ax} bond length is shown together with that calculated for **1** (where the axial dimethylbenzimidazole ligand is conserved), which has been discussed above. For both curves, the reaction energy at the optimized bond distance in the six-coordinate compound has been set as the origin of the energy (2.29 Å for **1** and 2.23 Å for **1′**). The absolute BDE in the gas phase for **1′** at this Co−N_{ax} distance is 214.4 kcal/mol. It can be observed that the two curves are very similar. A shortening of the Co−N_{ax} bond to 2.0 Å leads to an increase in the reaction energy of 7.2 kcal/mol in **1′** compared to 8.8 kcal/mol in **1**. A lengthening to 2.6 Å lowers the reaction energy of **1′** by 10.1 kcal/mol whereas that of **1** is lowered by 8.1 kcal/mol. The trend is therefore the same for both compounds. These results indicate that the substitution of the axial ligand of cobalamin by a histidine residue, which is observed in enzymes that depend on methylcobalamin, does not alter the relationship between the bond distance and the electronic trans effect of the axial base on the Co−C bond cleavage.

Formation of cob(III)alamin. Figure 6 shows the dependence of the bond dissociation energy for type B heterolysis for both compounds, **1′** and **1**, on the Co−N_{ax} bond length. As before, the values for the optimized distance in the six-coordinate compound have been chosen as the origin of the energy (263.1 kcal/mol for **1′**). It becomes clear that the substitution of the axial ligand has hardly any influence on this type of heterolysis. The two curves are practically parallel. A shortening of the Co−N_{ax} bond to 2.0 Å leads to a decrease in the reaction energy of 10.2 kcal/mol in **1′** compared to 12.9 kcal/mol in **1**. Upon lengthening of the Co−N_{ax} bond to 2.6 Å, the bond dissociation of **1′** increases by 9.7 kcal/mol, and that of **1**, by 7.8 kcal/mol. Again, this confirms that conclusions obtained from studies of the trans influence of imidazole can be safely extrapolated to histidine.

Larger Basis Set Calculations. To check the validity of the rather small basis set (I) used in this work, some single-point calculations have been carried out with the larger basis set (II). Because of the smaller size of the system, these tests have been carried out with histidine as the axial ligand. The reaction energy for both types of heterolytic Co−C cleavage has been calculated at Co−N_{ax} distances of 2.23, 2.0, and 2.6 Å, and the values have been compared to those obtained with the smaller basis set.

Table 3 shows the results calculated with both the smaller basis set (I) and the larger basis set (II) for both types of Co−C bond heterolysis, where the reaction energy at the optimized Co−N_{ax} distance of 2.23 Å has been set to zero. It can be seen

TABLE 3: Effect of the Basis Set on the Dependence of the Reaction Energy on the Co−N_{Ax} Distance[a]

R(Co−N_{ax})	2.0 Å		2.6 Å	
basis set	I	II	I	II
heterolysis type A	+7.2	+5.4	−10.1	−9.3
heterolysis type B	−10.2	−11.5	+12.7	+13.6

[a] Values are given relative to the BDE at R(Co−N_{Ax}) = 2.23 Å, which is taken as zero.

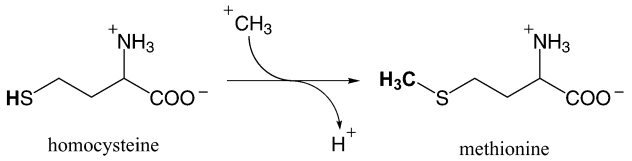

Figure 9. Reaction catalyzed by methionine synthase.

that the relative reaction energies obtained with the larger basis set show the same trend as those calculated with the smaller one. The results differ by less than 2 kcal/mol.

3.4. Influence of the Substrate and the Solvent on the Thermodynamics of the Reaction. The reaction energy in the gas phase calculated for both types of Co−C bond heterolysis is extremely high. This is due to the fact that the charged species formed in these reactions are highly unstable in the gas phase. In the enzymes that use methylcobalamin as a cofactor, however, the methyl cation formed in the first reaction step does not stay as such but is transferred to the substrate. Figure 9 shows the methylation of homocysteine to give methionine as it takes place in the enzyme methionine synthase. Also, it has to be taken into account that the substrate before entering the enzyme and the product after its release are solvated. These effects, which have not been taken into account in the present work and which would require much more sophisticated calculations, should lower the computed absolute BDE dramatically, bringing it to a value compatible with a biological environment. However, these values are not relevant to the study of the dependence of the BDE on the Co−N_{ax} bond length, as they will lower the energy of all optimized product states by a constant term, independently of the Co−N_{ax} distance, and the relative BDE would be unchanged.

3.5. Adenosylcobalamin. The reaction modes of methyl and adenosylcobalamin in the enzymatic environment are very different. To evaluate how the influence of the axial ligand on the heterolytic Co−C bond cleavage depends on the electronic character of the alkyl ligand, additional calculations have been performed on a larger system in which the methyl ligand has been replaced by tetrahydrofuran attached to the Co−CH_2− group. This system should be a valid model for the electronic effects of adenosylcobalamin, as they are supposed to come mainly from the tetrahydrofuran ring. Figure 8 shows the structure of [Co(Cor)(Benz)(CH_3R)] (R = tetrahydrofuran) (**1″**), which has been fully optimized in the singlet electronic state at the Becke3LYP level of theory. The geometric parameters of **1″** have been discussed previously.[45] They are very similar to those computed for **1**, the only important difference being the Co−N_{ax} distance that is 0.16 Å longer (2.45 Å in **1″** vs 2.29 Å in **1**).

The reaction energy for both heterolytic Co−C bond cleavage processes in **1″** has been calculated as the energy of reactions

$$\mathbf{1''}(\text{frozen } R(\text{Co}-\text{N}_{ax}))^{+} \rightarrow \mathbf{3}(\text{frozen } R(\text{Co}-\text{N}_{ax})) + \text{CH}_2\text{C}_4\text{OH}_7^{+}$$

and

$$\mathbf{1''}(\text{frozen } R(\text{Co}-\text{N}_{ax}))^{+} \rightarrow \mathbf{4}(\text{frozen R}(\text{Co}-\text{N}_{ax}))^{2+} + \text{CH}_2\text{C}_4\text{OH}_7^{-}$$

as has been previously described for **1**. The reaction energy for the formation of cob(I)alamin (**3**) has been calculated at the optimized Co−N_{ax} distance of 2.45 Å as well as at Co−N_{ax} distances of 2.0, 2.2, 2.6, and 2.8 Å. The formation of cob(III)alamin (**4**) has been studied at Co−N_{ax} distances of 1.8, 1.93 (the optimized value for **4**), 2.0, 2.2, and 2.45 Å.

The results of the calculations performed on **1″** are largely the same as those obtained for methyl compound **1**.

Formation of cob(I)alamin. With respect to type A heterolysis, which is the operation mode of methylcobalamin in biological systems, the same trend that has been discussed for **1** can be observed for **1″**. Upon shortening of the Co−N_{ax} distance, the reaction energy for the formation of cob(I)alamin (**3**) increases, and it decreases when the Co−N_{ax} distance is lengthened. The effect of a shortening of the Co−N_{ax} distance is nearly the same in **1** and in **1″**. In **1″**, a shortening of 0.45 Å leads to an increase in the BDE of 10.9 kcal/mol compared to an increase of 10.7 kcal/mol upon a shortening of 0.5 Å in **1**. The effect of a lengthening of the Co−N_{ax} distance is less pronounced in **1″** than in **1**. In **1″**, a lengthening of 0.35 Å lowers the BDE by 5.3 kcal/mol, whereas in **1** a lengthening of 0.3 Å provokes a decrease in the BDE of 8.1 kcal/mol. The trend, however, is the same in both compounds. This indicates that the different behavior of methylcobalamin and adenosylcobalamin in biological systems is not due to a different response to the axial ligand, and the results of the calculations on the trans effect in methylcobalamin can safely be extrapolated to adenosylcobalamin.

Formation of cob(III)alamin. The Co−C bond heterolysis in which both electrons are left on the alkyl group and five-coordinate cob(III)alamin is formed appears to be a competitive reaction for Co−C bond homolysis in free adenosylcobalamin. The same dependence of the BDE on the Co−N_{ax} distance that has been found for methylcobalamin (**1**) can be observed in our model for adenosylcobalamin (**1″**). A shortening of the bond between cobalt and the axial benzimidazole strongly favors Co−C bond heterolysis. Because of the larger difference between the optimized Co−N_{ax} distances in **1″** and **4** (2.45 vs 1.93 Å), this effect is more pronounced in **1″** than in **1**. A shortening of the Co−N_{ax} distance in **1″** of 0.25 Å (2.20 instead of 2.45 Å) lowers the Co−C BDE by 10.54 kcal/mol. Further shortening of the Co−N_{ax} bond to 1.80 Å leads to a 33.5 kcal/mol decrease in the reaction energy for type B heterolysis.

4. Simple Molecular Orbital Explanation

The finding of such a substantially different effect of the distance of the trans axial base from the Co in the homolysis and both types of heterolysis of the Co−C bond prompted us to determine which one is the origin of this difference. The explanation happens to result quite simply from the analysis of the molecular orbitals.

The main electronic interaction between the axial base and the cobalt center is the formal donation from the free electron pair on the nitrogen to a metal orbital in the appropriate orientation. This will be along the z axis if the axes are those depicted in Figure 10. The only cobalt orbitals with the appropriate symmetry are $3d_{z^2}$ and $4p_z$. Population analysis shows, in fact, that the main changes take place in $3d_{z^2}$, so the discussion will concentrate on the Mulliken population of this orbital.

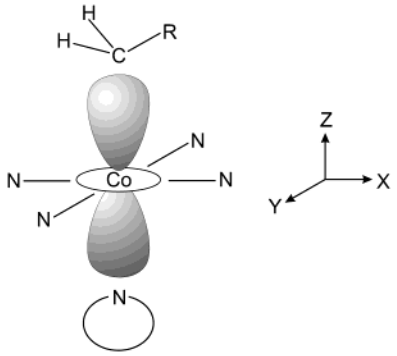

Figure 10. Scheme of the d_{z^2} orbital of Co involved in the Co−C and Co−N_{ax} bonds.

The donation from the axial base to the $3d_{z^2}$ orbital will depend critically on the occupation of that orbital, and this value changes dramatically for the different compounds considered. In the case of six-coordinate complex **1**, the Mulliken population in this orbital is 1.06 electrons, far from the ideal charge of 0.00 expected for a pure ionic Co(III) species but logical when taking into account the electron donation from the ligand orbitals. Five-coordinate complex **2**, produced by the elimination of a methyl radical CH_3• from **1**, has a charge of 1.10 electrons in this orbital. This is quite close to the expected 1 electron for this Co(II) species and reflects the fact that the methyl in **1** is actually quite close to neutral. The more relevant aspect of this result to the current discussion is, however, the very similar occupation of $3d_{z^2}$ in **1** and **2**. As a result, both complexes will have a similar response to displacements of the axial base, and the bond energy for homolysis will be essentially unchanged by this movement.

Things are very different when one considers the products of both heterolyses A and B. The product of heterolysis A is complex **3**(base-off), and a related complex with the Co−N_{ax} fixed at 2.29 Å was computed. The charge in the $3d_{z^2}$ orbital of this complex was 1.85. This is consistent with the full orbital one expects for this Co(I) species but with the important consequence that donation from the axial base to this full orbital is heavily disfavored. This is the reason that **3**(base-off) prefers to be four-coordinate and that heterolysis A is favored by long Co−N_{ax} distances. Things are just the opposite for heterolysis B. In this case, product **4** has a formal occupation of 0.69 in the $3d_{z^2}$ orbital, and donation from the base to this emptier orbital is favored. Because of this, the optimal Co−N_{ax} distance is shorter, and heterolysis B is favored by short Co−N_{ax} distances.

In view of this simple reasoning, which can be made from qualitative considerations, one may wonder if the high-level calculations presented throughout this article were necessary. The answer is that they were. This qualitative reasoning can predict the trends but gives little clue of their importance. For instance, it could be said a priori that a long Co−N_{ax} distance would favor heterolysis B, but the order of magnitude of this effect could not be predicted. The more quantitative analysis requires high-level calculations, and they are the only ones that are able to show that the effect of the axial base is chemically significant for heterolysis but not for homolysis.

5. Discussion

Implications for Enzymes Based On Coenzyme B_{12}. These enzymes react through homolytic cleavage of the Co−C bond. We have previously shown[45] that the distance of the axial base from the cobalt has little direct effect on the thermodynamics or kinetics of this reaction. Nevertheless, homolysis is not the only possible reaction for the Co−C bond in cobalamins. This bond can also undergo either of the two types of heterolytic cleavage described above. The results of our calculations, showing that both heterolysis reactions are highly sensitive to the Co−N_{ax} distance, indicate that the axial base can play an important role in modulating the competition among the three possible reactions in enzymes based on coenzyme B_{12}.

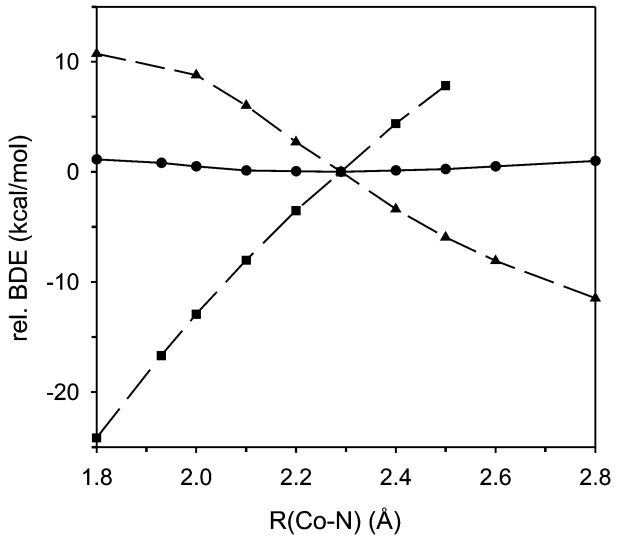

Figure 11. Relative Co−C bond dissociation energy (in kcal/mol) for Co−C bond homolysis (−), heterolysis with the formation of **3** (−▲−), and heterolysis with the formation of **4** (−■−) as a function of the Co−N_{ax} distance (in Å). The bond dissociation energies at the optimal Co−N_{ax} distance in **1** (2.29 Å) have been chosen as zero. The absolute values at this point are 22.9 kcal/mol for homolysis, 211.2 kcal/mol for the formation of **3**, and 262.9 kcal/mol for the formation of **4**.

Figure 11 shows a comparison of the dependence of the Co−C BDE on the Co−N_{ax} distance for homolysis (solid line) and the two different modes of heterolysis that lead to the formation of cob(I)alamin (dashed line, triangles) and cob(III)-alamin (dashed line, squares), respectively. It becomes obvious that whereas homolysis is practically independent of the Co−N distance this is by no means the case for heterolysis. Lengthening of the Co−N_{ax} distance clearly favors a heterolytic cleavage of the Co−C bond such that both electrons are left on cobalt to form cob(I)alamin and CH_3^+. However, if the Co−N_{ax} distance becomes too short, then the undesired formation of five-coordinate cob(III)alamin is facilitated.

Our results indicate thus that, despite the absence of the direct influence of the axial ligand on Co−C bond homolysis, the distance between this ligand and the metal center can be crucial in preventing the heterolysis reaction. In enzymes carrying out homolysis, the cofactor must be in a base-on form to prevent type A heterolysis. Moreover, the axial ligand must be a relatively long distance from the metal center because if it were too close the undesired type B heterolysis, resulting in the formation of five-coordinate cob(III)alamin, would take place.

This observation is consistent with the crystallographic evidence indicating that in all enzymes containing coenzyme B_{12} the cobalamin is bound to an axial base—either the dimethylbenzimidazole itself, as in diol hydratase,[49] or a histidine amino acid from the protein chain, as in glutamate mutase,[71] and methylmalonyl-CoA mutase.[4,72−74] Crystallographic data also predict a long Co−N_{ax} distance in the protein environment, with values such as 2.34,[71] 2.47,[72] 2.48,[73] 2.49,[73] and 2.50 Å.[49] The replacement of benzimidazole by histidine does not seem very significant from an electronic point of

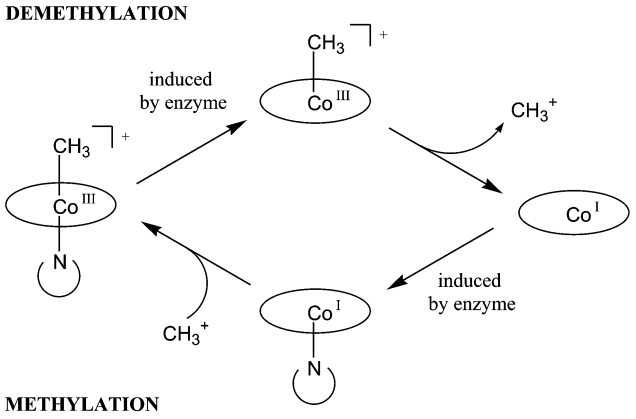

Figure 12. Possible role of the axial ligand in enzymatic catalysis with methylcobalamin as a cofactor.

view,[45] but the presence of a long distance between cobalt and the axial base appears to be critical.

Our results therefore support previous proposals based mainly on experimental data, stating that nature uses the axial ligands in adenosylcobalamin-dependent enzymes to prevent the undesirable heterolysis reaction.[12,15,66−68,75,76] The idea of the role of the trans ligand in preventing the coenzyme from participating in undesired side reactions has recently received support from the observation that substitution of the axial benzimidazole by a cyanide ligand leads to type B heterolysis of the Co−C bond.[69] Cyanide is a very strong σ-electron donor. Exchange of benzimidazole for cyanide therefore has the same effect as a shortening of the Co−N_{axial} bond: the electron density on cobalt is increased.

Implications for Enzymes Based on Methylcobalamin. These enzymes react through heterolytic cleavage of the Co−C bond. They undergo a reaction of type A, leading to the formation of cob(I)alamin and CH_3^+. Our calculations have shown that this reaction depends very heavily on the distance of the axial base from the Co. In particular, the lengthening of the Co−N_{ax} distance favors the reaction, as shown in Figure 4. Consequently, product formation is optimally favored in the absence of an axial ligand. The fact that the only enzymes where the B_{12} cofactor is found in the base-off form are the iron−sulfur proteins in methanogens and acetogens,[52] which produce heterolytic Co−C bond cleavage, supports this observation.

The fact that the X-ray structure of the methylcobalamin-dependent human enzyme methionine synthase shows a histidine residue of a protein side chain coordinated to cobalt[6] could be seen as evidence against these considerations. However, we believe that, on the contrary, it points to a more elaborate role of the axial base in modulating the reactivity of the cofactor. The enzyme, as a catalyst, must perform a reaction cycle switching between two states—one with methylated cobalt (left side of reaction A) and another with the demethylated cobalt (right side of reaction A). The possibility that the position of a histidine amino acid on the protein chain can affect this equilibrium is quite appealing and points to a possible mechanism of the type depicted in Figure 12. In fact, the role of the axial histidine favoring the recovery of the methylcobalamin has been proposed from experimental data.[5,6,14,15,77−80]

The fact that the axial histidine is included in a His-Asp-Ser triad that could trigger the transformation of imidazole into imidazolato through protonation also supports the potential active role of the axial base in changing the methyl affinity of the cofactor depending of the stage of the reaction. These mechanistic proposals thus receive support from the current calculations.

6. Concluding Remarks

Becke3LYP calculations on $[Co(Cor)(Benz)(R)]^+$ and its products from the three possible dissociation processes of the Co−C bond show a sharply different dependence on the distance of the trans axial base from the cobalt. In the homolytic cleavage leading to cob(II)alamin, the dissociation process is essentially unaffected by changes in the position of the trans axial ligand; the heterolytic dissociation leading to cob(I)alamin, which is also present in biological systems, is heavily favored by long Co−N_{ax} distances; and the heterolytic dissociation leading to cob(III)alamin is strongly favored by short Co−N_{ax} distances.

Calculations on $[Co(Cor)(Im)(CH_3)]^+$ and the products of its heterolysis show that the substitution of the dimethylbenzimidazole ligand by a histidine residue, which takes place in some enzymes, does not affect the behavior of the cofactor.

These results have important implications for the role of the trans axial ligand for both types of B_{12} cofactors. For B_{12} coenzymes reacting through homolysis, these results indicate that the axial ligand must remain present throughout the reaction, though a relatively long distance from the metal, to prevent the system from undergoing heterolysis. For methylcobalamins involved in heterolytic cleavage yielding CH_3^+, these results suggest that the axial ligand can play an active role in the enzymatic process, approaching the cobalt center when the methyl must be attached and moving away from the metal when the methyl must be released.

Acknowledgment. Financial support from the Spanish DGES (project no. PB98-0916-C02-01) and the Catalan DURSI (project no. 1999 SGR00089) is acknowledged. F.M. is also grateful for the support of DURSI.

References and Notes

(1) Kräutler, B.; Arigoni, D.; Golding, B. T. *Vitamin B_{12} and B_{12}-Proteins*; Wiley-VCH: Weinheim, Germany, 1998.
(2) Banerjee, R. *Chemistry and Biochemistry of B_{12}*; Marcel Dekker: New York, 1999.
(3) Buckel, W.; Golding, B. T. *Chem. Soc. Rev.* **1996**, *26*, 329.
(4) Mancia, F.; Keep, N. H.; Nakagawa, A.; Leadlay, P.; McSweeney, S.; Rasmussen, B.; Bösecke, P.; Diat, O.; Evans, P. R. *Structure* **1996**, *4*, 339.
(5) Matthews, R. G. *Acc. Chem. Res.* **2001**, *34*, 681.
(6) Drennan, C. L.; Huang, S.; Drummond, J. T.; Matthews, R. G.; Ludwig, M. L. *Science (Washington, D.C.)* **1994**, *266*, 1669.
(7) Dong, S.; Padmakumar, R.; Banerjee, R.; Spiro, T. G. *J. Am. Chem. Soc.* **1999**, *121*, 7063.
(8) Bandarian, V.; Matthews, R. G. *Biochemistry* **2001**, *40*, 5056.
(9) Magnusson, O. T.; Frey, P. A. *J. Am. Chem. Soc.* **2000**, *122*, 8807.
(10) Fasching, M.; Schmidt, W.; Kräutler, B.; Stupperich, E.; Schmidt, A.; Kratky, C. *Helv. Chim. Acta* **2000**, *83*, 2295.
(11) Randaccio, L. *Comments Inorg. Chem.* **1999**, *21*, 327.
(12) Sirovatka, J. M.; Finke, R. G. *J. Am. Chem. Soc.* **1997**, *119*, 3057.
(13) Cregan, A. G.; Brasch, N. E.; van Eldik, R. *Inorg. Chem.* **2001**, *40*, 1430.
(14) Seravalli, J.; Brown, K. L.; Ragsdale, S. W. *J. Am. Chem. Soc.* **2001**, *123*, 1786.
(15) Marzilli, L. G. In *Bioinorganic Catalysis*, 2nd ed.; Reedijk, J., Bouwman, E., Eds.; Marcel Dekker: New York, 1999; pp 423−468.
(16) Hung, R. R.; Grabowski, J. J. *J. Am. Chem. Soc.* **1999**, *121*, 1359.
(17) Maiti, N.; Widjana, L.; Banerjee, R. *J. Biol. Chem.* **1999**, *274*, 3233.
(18) Fonda, E.; Michalowicz, A.; Randaccio, L.; Tauzher, G.; Vlaic, G. *Eur. J. Inorg. Chem.* **2001**, *5*, 1269.
(19) Trommel, J. S.; Warncke, K.; Marzilli, L. G. *J. Am. Chem. Soc.* **2001**, *123*, 3358.
(20) Shian, J. J.; Walker, L. A.; Anderson, N. A.; Cole, A. G.; Sension, R. J. *J. Phys. Chem. B* **1999**, *103*, 10532.
(21) Scheuring, E.; Padmakumar, R.; Banerjee, R.; Chance, M. R. *J. Am. Chem. Soc.* **1997**, *119*, 12192.
(22) Champloy, F.; Jogl, G.; Reitzer, R.; Buckel, W.; Bothe, H.; Beatrix, B.; Broeker, G.; Michalowicz, A.; Meyer-Klaucke, W.; Kratky, C. *J. Am. Chem. Soc.* **1999**, *121*, 11780.
(23) Sirovatka, J. M.; Finke, R. G. *Inorg. Chem.* **1999**, *38*, 1697.
(24) Cini, R.; Moore, S. J.; Marzilli, L. G. *Inorg. Chem.* **1998**, *37*, 6890.

(25) Marques, H. M.; Brown, K. L. *Coord. Chem. Rev.* **1999**, *190*−*192*, 127.
(26) Geremia, S.; Calligaris, M.; Randaccio, L. *Eur. J. Inorg. Chem.* **1999**, *6*, 981.
(27) Sirovatka, J. M.; Rappé, A. K.; Finke, R. G. *Inorg. Chim. Acta* **2000**, *300*, 545.
(28) Marques, H. M.; Ngoma, B.; Egan, T. J.; Brown, K. L. *J. Mol. Struct.: THEOCHEM* **2001**, *561*, 71.
(29) Marques, H. M.; Brown, K. L. *Coord. Chem. Rev.* **2002**, *225*, 123.
(30) Siegbahn, P. E. M.; Blomberg, M. R. A. *Chem. Rev.* **2000**, *100*, 421.
(31) Christianson, D. W.; Lipscomb, W. N. *J. Am. Chem. Soc.* **1985**, *107*, 2682.
(32) Mealli, C.; Sabat, M.; Marzilli, L. G. *J. Am. Chem. Soc.* **1987**, *109*, 1593.
(33) Zhu, L.; Kostic, N. M. *Inorg. Chem.* **1987**, *26*, 4194.
(34) Hansen, L. M.; Kumar, P. N. V. P.; Marynick, D. S. *Inorg. Chem.* **1994**, *33*, 728.
(35) Torrent, M.; Musaev, D. G.; Morokuma, K.; Ke, S.-C.; Warncke, K. *J. Phys. Chem. B* **1999**, *103*, 8618.
(36) Ke, S.-C.; Torrent, M.; Musaev, D. G.; Morokuma, K.; Warncke, K. *Biochemistry* **1999**, *38*, 12681.
(37) George, P.; Siegbahn, P. E.; Glusker, J. P.; Bock, C. W. *J. Phys. Chem. B* **1999**, *103*, 7531.
(38) Smith, D. M.; Golding, B. T.; Radom, L. *J. Am. Chem. Soc.* **1999**, *121*, 9388.
(39) Wetmore, S. D.; Smith, D. M.; Radom, L. *J. Am. Chem. Soc.* **2000**, *122*, 3403.
(40) Smith, D. M.; Golding, B. T.; Radom, L. *J. Am. Chem. Soc.* **2001**, *123*, 1664.
(41) Jensen, K. P.; Sauer, S. P. A.; Liljefors, T.; Norrby, P.-O. *Organometallics* **2001**, *20*, 550.
(42) Andruniow, T.; Zgierski, M. Z.; Kozlowski, P. M. *J. Phys. Chem. B* **2000**, *104*, 10921.
(43) Andruniow, T.; Zgierski, M. Z.; Kozlowski, P. M. *Chem. Phys. Lett.* **2000**, *331*, 509.
(44) Andruniow, T.; Zgierski, M. Z.; Kozlowski, P. M. *J. Am. Chem. Soc.* **2001**, *123*, 2679.
(45) Dölker, N.; Maseras, F.; Lledós, A. *J. Phys. Chem. B* **2001**, *105*, 7564.
(46) Dong, S.; Padmakumar, R.; Banerjee, R.; Spiro, T. G. *J. Am. Chem. Soc.* **1998**, *120*, 9947.
(47) Randaccio, L.; Geremia, S.; Sterner, M.; Toffoli, D.; Zangrando, E. *Eur. J. Inorg. Chem.* **2002**, 93.
(48) Yamanishi, M.; Yamada, S.; Muguruma, H.; Murakami, Y.; Tobimatsu, T.; Ishida, A.; Yamauchi, J.; Toraya, T. *Biochemistry* **1998**, *37*, 4799.
(49) Shibata, N.; Masuda, J.; Tobimatsu, T.; Toraya, T.; Suto, K.; Morimoto, Y.; Yasuoka, N. *Structure* **1999**, *7*, 997.
(50) Lawrence, C. C.; Gerfen, G. J.; Samano, V.; Nitsche, R.; Robins, M.; Retey, J.; Stubbe, J. *J. Biol. Chem.* **1999**, *274*, 7039.
(51) Reitzer, R.; Gruber, K.; Jogl, G.; Wagenr, U. G.; Bothe, H.; Buckel, W.; Kratky, C. *Structure* **1999**, *7*, 891.
(52) Ragsdale, S. W.; Lindahl, P. A.; Mück, E. *J. Biol. Chem.* **1987**, *262*, 14289.
(53) Doukov, T.; Seravalli, J.; Ragsdale, S. W. *Structure* **2000**, *8*, 817.
(54) Wirt, M. D.; Kumar, M.; Wu, J.-J.; Scheuring, E. M.; Ragsdale, S.; Chance, M. *Biochemistry* **1995**, *34*, 5269.
(55) Jensen, M. P.; Halpern, J. *J. Am. Chem. Soc.* **1999**, *121*, 2181.
(56) Becke, A. D. *J. Chem. Phys.* **1993**, *98*, 1372.
(57) Becke, A. D. *J. Chem. Phys.* **1993**, *98*, 5648.
(58) Lee, C.; Yang, W.; Parr, G. *Phys. Rev. B* **1988**, *37*, 385.
(59) Stephens, P. J.; Devlin, F. J.; Chabalowski, C. F.; Frisch, M. J. J. *J. Phys. Chem.* **1994**, *98*, 11623.
(60) Hay, P. J.; Wadt, W. R. *J. Chem. Phys.* **1985**, *82*, 299.
(61) Hehre, W. J.; Ditchfield, R.; Pople, J. A. *J. Chem. Phys.* **1972**, *56*, 2257.
(62) Hariharan, P. C.; Pople, J. A. *Theor. Chim. Acta* **1973**, *28*, 213.
(63) Hehre, W. J.; Steward, R. W.; Pople, J. A. *J. Chem. Phys.* **1969**, *51*, 2657.
(64) Ehlers, A. W.; Böhme, M.; Dapprich, S.; Gobbi, A.; Höllwarth, A.; Jonas, V.; Köhler, K. F.; Stegmann, R.; Veldkamp, A.; Frenking, G. *Chem. Phys. Lett.* **1993**, *208*, 111.
(65) Frisch, M. J.; Trucks, G. W.; Schlegel, H. B.; Scuseria, G. E.; Robb, M. A.; Cheeseman, J. R.; Zakrzewski, V. G.; Montgomery, J. A., Jr.; Stratmann, R. E.; Burant, J. C.; Dapprich, S.; Millam, J. M.; Daniels, A. D.; Kudin, K. N.; Strain, M. C.; Farkas, O.; Tomasi, J.; Barone, V.; Cossi, M.; Cammi, R.; Mennucci, B.; Pomelli, C.; Adamo, C.; Clifford, S.; Ochterski, J.; Petersson, G. A.; Ayala, P. Y.; Cui, Q.; Morokuma, K.; Malick, D. K.; Rabuck, A. D.; Raghavachari, K.; Foresman, J. B.; Cioslowski, J.; Ortiz, J. V.; Stefanov, B. B.; Liu, G.; Liashenko, A.; Piskorz, P.; Komaromi, I.; Gomperts, R.; Martin, R. L.; Fox, D. J.; Keith, T.; Al-Laham, M. A.; Peng, C. Y.; Nanayakkara, A.; Gonzalez, C.; Challacombe, M.; Gill, P. M. W.; Johnson, B. G.; Chen, W.; Wong, M. W.; Andres, J. L.; Head-Gordon, M.; Replogle, E. S.; Pople, J. A. *Gaussian 98*, revision A.3; Gaussian, Inc.: Pittsburgh, PA, 1998.
(66) Garr, C. D.; Sirovatka, J. M.; Finke, R. G. *J. Am. Chem. Soc.* **1996**, *118*, 11142.
(67) Toraya, T.; Ishida, A. *J. Biol. Chem.* **1991**, *266*, 5430.
(68) Ishida, A.; Toraya, T. *Biochemistry* **1993**, *32*, 1535.
(69) Brasch, N. E.; Haupt, R. J. *Inorg. Chem.* **2000**, *39*, 5469.
(70) Martin, B. D.; Finke, R. G. *J. Am. Chem. Soc.* **1990**, *112*, 2419.
(71) Krasser, R.; Jogl, M.; Buckel, G.; Bothe, W.; Kratky, H. *Acta Crystallogr., Sect. D* **1998**, *54*, 1039.
(72) Mancia, F.; Evans, P. R. *Structure* **1998**, *6*, 711.
(73) Mancia, F.; Evans, P. R. *Biochemistry* **1999**, *38*, 7999.
(74) Thoma, N. H.; Evans, P. R.; Leadlay, P. F. *Biochemistry* **2000**, *39*, 9213.
(75) Garr, C. D.; Sirovatka, J. M.; Finke, R. G. *Inorg. Chem.* **1996**, *35*, 5912.
(76) Marzilli, L. G.; Summers, M. F.; Bresciani-Pahor, N.; Zangrando, E.; Charland, J.-P.; Randaccio, L. *J. Am. Chem. Soc.* **1985**, *107*, 6880.
(77) Ludwig, M. L.; Drennan, C. L.; Matthews, R. G. *Structure* **1996**, *4*, 505.
(78) Ludwig, M. L.; Matthews, R. G. *Annu. Rev. Biochem.* **1997**, *66*, 269.
(79) Jarrett, J. T.; Amaratunga, M.; Drennan, C. L.; Scholten, J. D.; Sands, R. H.; Ludwig, M. L.; Matthews, R. G. *Biochemistry* **1996**, *35*, 2464.
(80) Ludwig, M. L.; Matthews, R. G. *Annu. Rev. Biochem.* **1997**, *66*, 269.
(81) Rossi, M.; Glusker, J. P.; Randaccio, L.; Summers, M. F.; Toscano, P. J.; Marzilli, L. G. *J. Am. Chem. Soc.* **1985**, *107*, 1729.